

# Durability Mechanics of Calcium Leaching of Concrete and Beyond

F.-J.Ulm, F.H.Heukamp, & J.T.Germaine  
*Massachusetts Institute of Technology, Cambridge, Massachusetts*

**ABSTRACT:** In recent years, Durability Mechanics emerged as a new discipline of Engineering Mechanics, driven by the rapid decay of our built infrastructure, and by some critical problems related to safe and economic hazardous waste storage. One critical problem in this field is calcium leaching of cementitious materials; and the progress made in this field may well improve health monitoring capabilities in other fields, such as durability problems in biological materials, related for instance to bone diseases as Osteoporosis. Focus of this paper is a review of recent results dealing with the strength properties and modeling of cementitious materials subjected to a severe chemical softening, which may well serve beyond.

## 1 INTRODUCTION

Osteoporosis, the 'silent epidemic', is a systemic skeletal disease characterized by low bone mass density (BMD) and microarchitectural deterioration of bone tissue. The socioeconomic effect of Osteoporosis is enormous. Recent estimations by the National Osteoporosis Foundation indicate that in 1996 approximately 29 million people aged over 50 in the United States either had osteoporosis or were at risk of developing the disease. This number is expected to be 41 million by the year 2015. In undegraded bone, a finely tuned cellular activity and frequency ensures a continuous remodeling of bone, repairing damage and fracture in the microstructure. This process is regulated by two types of cells: Resorbing cells, called osteoclasts, dissolve bone minerals (hydroxyapatite  $\text{Ca}_{10}[\text{PO}_4]_6[\text{OH}]_2$ ), and osteoblasts cells move into the space left by the osteoclasts, regenerating the collagenous micromorphology and the chemical boundary conditions for the re-mineralization of bone (Hellmich & Ulm, 2001). While the biochemomechanical deterioration of bone that leads to osteoporosis is still a matter of intensive research, it obviously results from a kinematic imbalance between osteoclast and osteoblast activity. With increasing age, the overall resorption rate is higher than the overall refilling rate, and this kinematic imbalance leads ultimately to an increased risk of bone fracture during downfall.

At first glance, concrete durability problems are

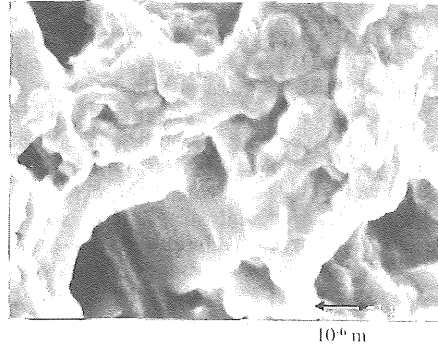


Figure 1: 'Bony' microstructure of calcium depleted cementitious materials (SEM Mag. 20k)

of a different kind: they are conditioned by heat- and mass transport phenomena, amplified in time and space by chemical reactions, which are coupled with deformation and fracture of the material. A typical example is Calcium leaching of cementitious materials, the reference design scenario of e.g. nuclear waste disposal structures, triggered by a lower Calcium concentration in the interstitial pore solution than some equilibrium Calcium concentration. The leaching of the Calcium from the matrix (Portlandite Crystals, C-S-H), leads to a significant loss of strength and stiffness, and the material becomes significantly pressure sensitive.

On second sight, osteoporosis and Calcium leaching of concrete materials have several things in common, starting from a 'bony' microstruc-

ture of Calcium leached cementitious materials, which shows strong similarity with osteoporotic bones (see figure 1); and progress in one field may well improve health monitoring capabilities in the other. Having this in mind, this paper reviews some recent results of research on Calcium leached cement-based material systems dealing with the strength properties and modeling of cementitious materials subjected to severe chemical softening.

## 2 THE TRIAXIAL STRENGTH DOMAIN OF CALCIUM LEACHED MATERIALS

The problem of mechanical integrity of concrete subjected to Calcium leaching is a field problem, related to the Calcium concentration in the solid phase, which is partially dissolved due to a Calcium concentration in the interstitial pore solution lower than the equilibrium concentration. In between two asymptotes (unleached versus Calcium depleted material), Calcium leaching leads to an increase of the porosity, but also to a change of the material properties of the remaining solid phase, and both are not uniformly distributed in the bulk material. In addition, the heterogeneous nature of cement-based composites (mortar, concrete, etc.) further complicates the assessment of the macroscopic strength domain: Calcium leaching mainly affects the cement paste matrix, and sometimes the interface, but rarely the aggregate. Experiments must be carried out on finite sized material specimens which contain sufficient matter in order to be representative of the macroscopic material behavior. The slowness of the degradation process requires artificially accelerated chemical aging conditions, to reach a representative state of degradation in a reasonable time of laboratory tests. On the other hand, given the various potential environmental boundary conditions, it is not sure whether a specific acceleration method is rep-

resentative of the 'real' Calcium leaching process, to which the material and structure will be subjected during its service life. This highlights the experimental difficulty of assessing the material performance of partially degraded material samples. One way to overcome this difficulty, is to assume a specific strength distribution in the material specimen, associated with a specific accessible solid Calcium concentration (Carde 1996; Carde et al. 1996; Le Bellego 2001). This approach, albeit efficient, has the disadvantage that the stress distribution is not unique, and hence the strength values found for a specific loading and degradation state may well not be representative for another one. For instance, it is not clear, whether the results from uniaxial strength and stiffness tests on partially degraded material specimens can be extrapolated to more realistic triaxial stress states. Another approach consists in determining the asymptotic strength behavior (undegraded versus degraded) of both the composite material and its components, and by applying some homogenization theories to evaluate the macroscopic strength domain.

### 2.1 Experimental Evidence

An extensive series of triaxial strength tests on undegraded and Calcium depleted cement pastes and mortars of water-cement ratio  $w/c = .5$  was performed. Samples were subjected to Calcium leaching using the accelerated leaching technique described in detail in Heukamp et al. 2001a, involving a highly concentrated Ammonium Nitrate solution (6M) in a slowly oscillating container, assuring good mixing conditions. The Calcium is leached incongruently, dissolving the Portlandite ( $Ca(OH)_2$ ) first and then decalcifying the Calcium Silicate Hydrates (CSH). The location corresponding to the Portlandite dissolution can be observed visually as a sharp color change and is referred to as the leaching front. At the chosen Ammonium Nitrate concentration, the front moves with  $x_d = 2\text{mm}/\sqrt{d}$  and reaches the middle of the specimen after about 9 days (the diameter being 11.5 mm). The complete Calcium depletion is finished after about 45 days, as XRF analysis shows. At this point, a uniformly Calcium leached sample is obtained. This is a necessity to separate the effects of still changing Calcium concentrations and the change in mechanical properties. In real life situations, water with different Calcium content will lead to different Calcium equilibrium concentrations in the cementitious material. The particularly severe leaching effect of the Ammonium Nitrate solution can be regarded as an asymptotic case of the effects of Calcium leaching on cementitious materials.

The triaxial strength tests were carried out with a high pressure cell equipped with an internal load cell and a pore pressure measurement device. All

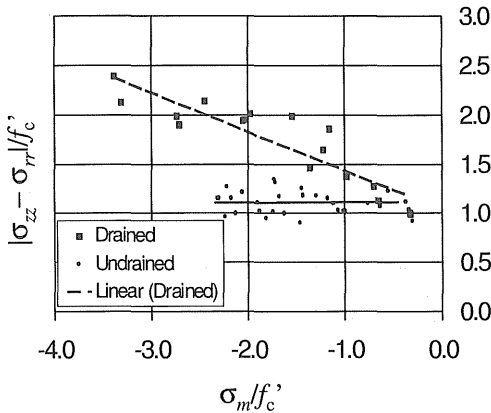


Figure 2: Triaxial Strength Domain of calcium leached cement paste ( $w/c = 0.5$ ).

tests were performed displacement driven. Vertical displacement, pore water pressure, change in pore water volume, cell pressure and vertical load were recorded with an automatic data acquisition system. Figure 2 shows the results of the triaxial tests on leached cement pastes in a  $(\sigma_{rr} - \sigma_{zz}) \times \sigma_m$  plane, normalized by the compressive strength, where  $\sigma_m = \frac{1}{3}(\sigma_{zz} + 2\sigma_{rr})$  is the mean stress,  $\sigma_{zz}$  the vertical applied stress, and  $\sigma_{rr} = \sigma_{\theta\theta}$  the horizontal stress. The different tests line up on a straight line, the slope of which indicates the friction capacity of the material. Table 1 summarizes the results in terms of the Drucker-Prager material parameters: the friction coefficient  $\delta$  and the cohesion  $k$  which is obtained by extrapolating the results to zero confinement pressures. The results show a great deal of consistency between undegraded and degraded samples:

- The cohesion of the cement paste is always greater than the one of the composite material (mortar), and the ratio  $k_{CP}/k_M$  is on the same order for both undegraded and degraded material specimens,  $k_{CP}/k_M \sim 1.7 - 1.9$ ; similarly the residual cohesion of both the cement paste and the mortar is on same order of

Table 1: Experimentally determined Drucker-Prager strength parameters of unleached and leached cement pastes (CP) and mortars (M) [Drained Tests].

	$k$ [MPa]		$\delta$ [°]	
	CP	M	CP	M
Undegraded	17.1	9.8	0.82	1.1
Leached	2.3	1.2	0.23	0.73

$$k_{CP}(0)/k_{CP}(\infty) \sim k_M(0)/k_M(\infty) \sim 12 - 13\% \text{ of its initial value.}$$

- The friction coefficient of the composite (mortar) is greater than the one of the cement paste, but this increase differs strongly for the undegraded and degraded samples. Furthermore, while Calcium leaching leads to a substantial reduction of the friction coefficient for both matrix (cement paste) and composite (mortar), this loss of frictional performance of the cement paste is well above the one of the mortar.
- The failure of all cement paste specimens, whether degraded or not, occurs very localized on shear planes; and for the mortar samples it is the same, except for Calcium leached mortars, for which failure occurs in the material bulk over more than half of the sample size.

Comparison of the yield surfaces shows a very interesting shift in behavior. Figures 3 and 4 display the two asymptotic material states (undegraded material, completely leached material) in the  $\sqrt{J_2} \times \sigma_m$ -plane. We note:

- For the undepleted materials (see fig. 3), the difference in strength between mortar and cement paste is small: the strength of the cement paste is slightly higher than the strength of the mortar for mean stresses greater than  $\sigma_m = -40$  MPa, and this may well be explained by the influence of the interfacial transition zone (ITZ): A zone of higher porosity and lower strength exists around the aggregates in mortars and concretes and reduces the macroscopic strength of these materials. Failure starts through cracking in the transition zone and at stress levels of about 70% of the ultimate strength of the composite, the stress concentrations at large voids in the cement paste initiate cracking. The cracks

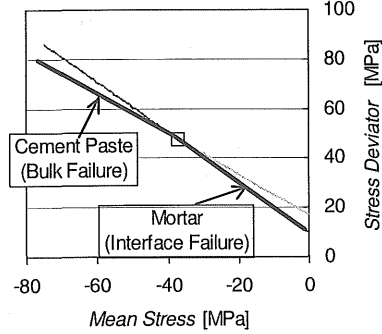


Figure 3: Strength domain of unleached composite (mortar) and matrix (cement paste).

spread with increasing stress and rejoin the cracks in the transition zone, starting to form the processing zone. The crack system then becomes continuous and the material fails.

- In the case of the Calcium leached mortars and paste as presented in figure 4, the picture is somehow different with a considerable difference in strength between mortar and cement paste. Only for low confinement pressures greater than  $\sigma_m = -2$  MPa, the cement paste exhibits a higher strength. On the other hand, as the confinement pressure increases ( $\sigma_m \leq -2$  MPa), the mortar is the material with the higher strength. This result is at least counter intuitive as it states that the strength of the composite material is actually greater than the strength of one of its constituents.

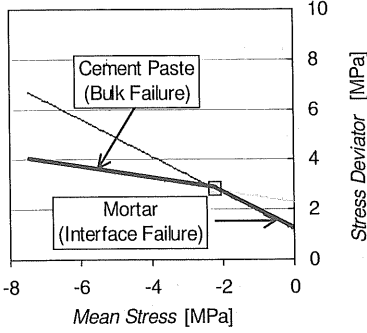


Figure 4: Strength domain of leached composite (mortar and matrix (cement paste)).

## 2.2 A Safe Lower Bound for Calcium Leached Cementitious Materials

The problem we consider here is the one of a matrix (cement paste) with spherical inclusions (sand particles). If the composite strength is larger than the matrix strength domain, the stress at a microscale of the spherical inclusions, say  $\sigma'_I$ , is required to be greater than the one prevailing in the matrix, say  $\sigma'_M$ . For a unit cell, composed of a matrix and an embedded spherical inclusion, with constant statically admissible stress fields, the stress field should be of the form (de Buhan & Taliercio 1991):

$$\sigma'_I = \sigma'_M + \delta\sigma_{ij}A_{ij} \quad (1)$$

where  $\delta\sigma_{ij}$  denote the excess in stress in the inclusion, with regard to the matrix stress  $e_i \cdot \sigma'_M \cdot e_j$ ; and the second order tensor  $A_{ij}$  of unit trace  $A_{ij} : 1 = 1$  is such that for any normal to the inclusion surface, say  $n$ , there is a continuity of the stress vector over the common interface:

$$t'_I(n) = \sigma'_I \cdot n \equiv \sigma'_M \cdot n = t'_M(n) \quad (2)$$

From (1) and (2) it follows for non-zero values of  $\delta\sigma_i$ :

$$\forall n; A_{ij} \cdot n = 0 \quad (3)$$

For spherical inclusions,  $n = e_r$ , and therefore:

$$A_{\theta\theta} = e_\theta \otimes e_\theta; A_{\varphi\varphi} = e_\varphi \otimes e_\varphi; A_{\theta\varphi} = e_\varphi \otimes e_\theta + e_\theta \otimes e_\varphi \quad (4)$$

Following the lower bound theorem of limit analysis, the stresses  $\sigma'_S$  and  $\sigma'_M$ , must satisfy the momentum balance equations in, and the strength criteria of both matrix and inclusion. However, for constant stress fields in the two material domains, the momentum balance in spherical coordinates reads:

$$\begin{aligned} 2\sigma_{rr} - \sigma_{\theta\theta} - \sigma_{\varphi\varphi} + \sigma_{r\theta} \cot \theta &= 0 \\ (\sigma_{\theta\theta} - \sigma_{\varphi\varphi}) + 3\sigma_{r\theta} \tan \theta &= 0 \\ 3\sigma_{r\varphi} + 2 \cot \theta \sigma_{\theta\varphi} &= 0 \end{aligned} \quad (5)$$

Therefore, to simultaneously satisfy Eqn. (5) in both material domains, it follows that the only spherical stress field which is constant in the two material domains, and which at the same time is statically admissible, is the macroscopic stress field; thus

$$\delta\sigma_{ij} = 0 \Leftrightarrow \sigma' = \sigma'_I = \sigma'_M \quad (6)$$

The immediate consequence of (6) is that a lower matrix strength cannot be enhanced by spherical inclusions, — in contrast to fiber reinforced composites (de Buhan & Taliercio 1991). Therefore, if we denote by  $F(\sigma')$  the macroscopic strength criterion, which defines the macroscopic strength domain  $D_{\text{hom}}$ , and by  $f_M, f_I$  and  $f_{\text{int}}$  the strength domain of the cement paste, of the aggregate inclusion, and of the common interface, the lower bound theorem of limit analysis, applied to the heterogeneous material system, implies that the actual strength domain is determined by the weakest material constituent of the system:

$$\sigma' \in D'_{\text{hom}} \Leftrightarrow F(\sigma') = \max(f_I, f_M, f_{\text{int}}) \leq 0 \quad (7)$$

For undegraded concrete materials, this can be attributed to the dominating role of the interfacial transition zone, which for normal strength concretes is found to be the weakest link in the material ( $F(\sigma') = f_{\text{int}}(t'_I(n) = t'_M(n))$ ). It has also been observed for undegraded high strength concrete materials, for which the limiting phase governing the overall strength behavior was found to be the aggregate ( $F(\sigma') = f_I(\sigma'_I)$ ). However, for Calcium depleted concrete materials, (7) just provides a lower bound of the experimentally observed macroscopic strength domain: for low confinement pressures, the overall strength is governed by the interfacial transition zone, which is accessible through triaxial tests on the composite material (here Calcium leached mortar). However, as the confinement pressure increases, (7) predicts that the behavior of the degraded cement paste governs the macroscopic strength domain, and therefore underestimates —as lower bound— the actual strength domain. Clearly, this indicates that a different mechanism is at work, which leads to a synergistic strengthening of the composite system beyond the particulate or matrix strength of its components. Observations of similar phenomena on other particulate composite systems exist in the literature (Ishai & Bodner 1970; Da Re 2000), but a good mechanism explaining this ultimate strength behavior has not been given —yet.

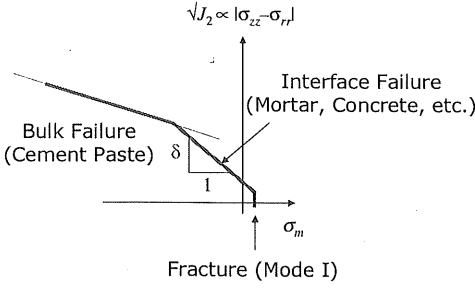


Figure 5: A 'safe' lower bound of the triaxial strength domain of calcium depleted cementitious materials.

Still, strength criterion (7) is an appropriate design strength criterion: it is a 'safe' lower bound of an accountable strength domain of 'chemically softened' cementitious materials. It still needs to be completed on the tension side, as sketched in figure 5. In between the limit states of the intact material and the degraded material, the strength domain needs to be interpolated. Chemoplasticity, or more precisely chemical softening, provides a reasonable means of interpolation.

### 2.3 Pressure Sensitivity of Calcium Leached Materials

A second important observation of the strength behavior of Calcium depleted cementitious materials is the increasing pore pressure sensitivity of these materials. This pressure sensitivity manifests itself through a high dependence of the strength behavior with regard to drained and undrained conditions. Figure 2 illustrates this behavior: the triaxial strength domain of Calcium leached cement pastes in undrained experiments is characterized by an almost zero frictional performance. Similar results were observed in undrained triaxial tests on Calcium depleted mortars. This pore pressure sensitivity has not been observed on intact cementitious material systems.

A first explanation of this behavior may refer to the effective stress concept of porous materials (Heukamp et al. 2001a). If we restrict ourselves to poroplastic evolutions, the Biot-Coussy theory of poromechanics delivers the stress and pressure state equations in the form:

$$\sigma_m = K_0 \epsilon - b p; \quad p = M(-b \epsilon + v_f) \quad (8)$$

where  $K_0$ ,  $b$  and  $M$  denote the drained bulk modulus, the Biot coefficient, and the Biot modulus;  $\epsilon = \text{tr} \boldsymbol{\epsilon}$  is the volume strain; and  $v_f$  is the fluid mass variation. The coefficients  $b$  and  $M$  can be assessed from (Coussy 1995):

$$b = 1 - \frac{K_0}{K_s}; \quad \frac{1}{M} = \frac{b - \phi_0}{K_s} + \frac{\phi_0}{K_f} \quad (9)$$

with  $\phi_0$  the initial porosity of the material,  $K_f$  the bulk modulus of the fluid and  $K_s$  the bulk modulus of the skeleton. The fluid bulk modulus is well known,  $K_f = 2.3$  GPa; while the skeleton bulk modulus  $K_s$  can be estimated from the homogenization theory that Kendall et al. (1983) applied to Young's modulus of porous materials:

$$K_0 = K_s(1 - \phi_0)^3 \quad (10)$$

In the case of an undrained experiment, for which the fluid mass variation is zero,  $v_f = 0$ , Eqn. (8), (9) and (10) give:

$$\begin{aligned} \frac{1}{B} &= - \left( \frac{p}{\sigma_m} \right)^{-1} = \frac{K_0}{M b} + b \\ &= 1 - \left( 1 - \frac{K_s}{K_f} \right) \frac{\phi_0(1 - \phi_0)^3}{1 - (1 - \phi_0)^3} \quad (11) \end{aligned}$$

$B = -p/\sigma_m$  is often referred to as compressibility coefficient or Skempton factor (Skempton 1954): it quantifies the amount of the macroscopically applied stress  $\sigma_m$  which is carried in an undrained test by the saturating fluid pressure. Figure 6 shows this function for two different  $K_s/K_f$ -ratio. The lower value,  $K_s/K_f = 3$ , corresponds roughly to the value of a degraded cement paste, the upper value  $K_s/K_f = 20$  to the one of the undegraded cement paste. The figure shows the two parameters which govern the pressure sensitivity of cementitious materials: the porosity  $\phi_0$  and the skeleton-to-fluid bulk modulus ratio  $K_s/K_f$ . The lower the  $K_s/K_f$ -ratio, the less sensitive is the function  $-p/\sigma_m$  to a change in initial porosity. This shows that the dominating parameter governing the pressure sensitivity of degraded cementitious materials is the  $K_s/K_f$ -ratio, associated with an intrinsic chemical damage of the solid part of

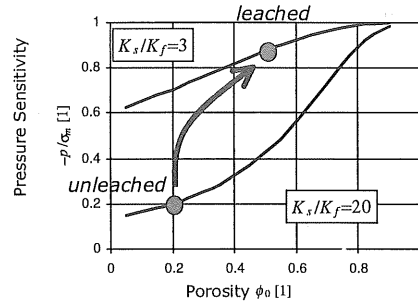


Figure 6: The two chemical damage mechanisms of calcium leaching: Increase of porosity; Intrinsic chemical damage of the remaining solid phase.

the microstructure. For a typical value of the initial porosity of the degraded material of  $\phi_0 = 0.5$ , the part of the total applied stress taken over by the pore pressure, is on the order of  $-p/\sigma_m = 90\%$ . This means that the 'effective' confinement stress  $\sigma'_m = \sigma_m + bp = 0.1\sigma_m$  in an undrained test, to which the chemically eroded skeleton is subjected, is small.

In summary, it appears that there are two distinct chemical damage mechanisms in Calcium depleted cementitious materials: one related to an increase of porosity, the other to a decrease of the skeleton-to-fluid bulk modulus ratio  $K_s/K_f$ ; but it is primarily the latter which leads to the high pressure sensitivity of Calcium leached materials. This sensitivity needs to be considered when designing concrete structures, subjected to leaching, for fast loading conditions (e.g. drop of a container), which approach undrained conditions. In this case, no frictional enhancement should be taken into account.

### 3 CHEMOPLASTICITY OF CALCIUM LEACHED MATERIALS

Chemoplasticity deals with the coupling between irreversible skeleton deformation and some chemical reactions affecting the skeleton behavior. For Calcium leaching, we may distinguish at least two relevant time scales of observation; one for short-term or accidental loading, in which the material behavior is affected by the presence of the fluid phase in the interstitial pore solution; the other for permanent loading, during which the material is simultaneously subjected to the Calcium leaching kinetics.

#### 3.1 Poroplasticity of Calcium Leached Materials

At the time scale of short-term loading, Calcium leached materials can be considered as saturated porous materials composed of a skeleton and a fluid phase saturating the pore space, as sketched in figure 7a. The fluid phase is a mixture, composed of a solvent and a solute, but at the time scale of the short-term loading the concentration of solvent and solute can be considered not to change. In other words, the problem does not involve the deterioration kinetics of Calcium leaching, and reduces to a poroplastic model. A 1D think model of poroplasticity is sketched in Figure 7b: a parallel spring–pressure cell device:  $\sigma_m$  is still the (volume) stress applied from the outside, which drives the deformation of the overall system, i.e. the strain  $\epsilon$ .  $\sigma_m$  is related to external forces applied to the system. In addition,  $p$  is the fluid pressure in the pore space, and due to an external supply of fluid mass the porosity changes, i.e.  $\phi - \phi_0$ , where  $\phi_0$  is the initial porosity. The external work applied to the system is the strain energy  $\sigma_m d\epsilon$  and the work

$pd\phi$  associated with a change in porosity, and the part of this work which is not stored in the skeleton in form of free energy  $\Psi_s$ , is dissipated into heat form:

$$\varphi dt = \sigma_m d\epsilon + pd\phi - d\Psi_s \geq 0 \quad (12)$$

From figure 7b, the free energy of the skeleton  $\Psi_s$  can be expressed as follows:

$$\Psi_s = \frac{1}{2} \left[ Mb^2 \left( \epsilon - \frac{1}{b}(\phi - \phi_0) \right)^2 + K_0(\epsilon - \epsilon^p)^2 \right] \quad (13)$$

where  $M = K_m/b^2 = bBK_u$ ; while all other material parameters, i.e.  $K_0, K_u$  = drained and undrained bulk modulus;  $b$  = Biot coefficient;  $B$  = Skempton coefficient, are defined by relations (9) to (11).  $\epsilon^p$  is the displacement of the friction element of strength  $k$ . Use of (13) in (12) yields:

$$\varphi dt = K_0(\epsilon - \epsilon^p)d\epsilon^p = (\sigma_m + bp)d\epsilon^p \geq 0 \quad (14)$$

together with:

$$\sigma_m = \frac{\partial \Psi_s}{\partial \epsilon} = K_0(\epsilon - \epsilon^p) - bp \quad (15)$$

$$p = \frac{\partial \Psi_s}{\partial \phi} = -M(b\epsilon - (\phi - \phi_0)) \quad (16)$$

Eq. (15) and (16) are the extension of the Biot's poroelastic static equations (8) to irreversible skeleton evolutions; and from (14) we identify the effective stress  $\sigma_m + bp$  as the driving force of irreversible skeleton deformation. From figure 7b, the plastically admissible stress and fluid pressure  $p$  are restrained by the following loading function:

$$F(\sigma_m, p) = |\sigma_m + bp| - k \leq 0 \quad (17)$$

Following the concepts of poroplasticity (Coussy 1995), a fluid pressure can lead to irreversible skeleton evolution, and the consistency condition gives:

$$dF = 0 \leftrightarrow d\sigma_m = -bdp : d\epsilon = d\epsilon^p = d\lambda \text{sign}(\sigma_m + bp) \quad (18)$$

$$d\phi = d\phi^p = d\lambda b \text{sign}(\sigma_m + bp) = b d\epsilon^p \quad (19)$$

where  $\phi^p$  is the plastic porosity, that is the irreversible change of porosity, and  $d\lambda$  is the plastic multiplier. Using (18) and (19) the dissipation can be rewritten in the form:

$$\varphi dt = \sigma_m d\epsilon^p + pd\phi^p \geq 0 \quad (20)$$

and the state equations read:

$$\sigma_m = \frac{\partial \Psi_s}{\partial \epsilon} = -\frac{\partial \Psi_s}{\partial \epsilon^p} = K_0(\epsilon - \epsilon^p) - bp \quad (21)$$

$$p = \frac{\partial \Psi_s}{\partial \phi} = -\frac{\partial \Psi_s}{\partial \phi^p} = -M [b(\epsilon - \epsilon^p) - (\phi - \phi^p)] \quad (22)$$

From (20) we formally identify the stress  $\sigma_m$  as the driving force of the plastic strain  $d\epsilon^p$ , and the fluid pressure  $p$  as the driving force of the plastic porosity  $d\phi^p$ . This identification enters the flow rules:

$$d\epsilon^p = d\lambda \frac{\partial F}{\partial \sigma_m}; \quad d\phi^p = \frac{\partial F}{\partial p} \quad (23)$$

The set of equations (20) to (22) and (17), are the constitutive equations of the 1D-poroplasticity model. They straightforwardly extend to three dimensions:

$$\varphi_1 dt = \sigma : d\epsilon_{ij}^p + pd\phi^p \geq 0 \quad (24)$$

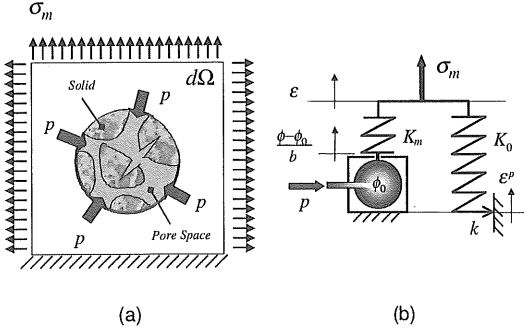


Figure 7: 1D-Think model of poroplasticity: (a) poromaterial; macroscopic material model.

$$\sigma = \frac{\partial \Psi_s}{\partial \epsilon} = -\frac{\partial \Psi_s}{\partial \epsilon^p}; \quad p = \frac{\partial \Psi_s}{\partial \phi} = -\frac{\partial \Psi_s}{\partial \phi^p} \quad (25)$$

and for a linear isotropic poroplastic material,

$$\sigma = \left( K_0 - \frac{2}{3}G \right) (\epsilon - \epsilon^p) 1 + 2G(\epsilon - \epsilon^p) - b(p - p_0) 1 \quad (26)$$

$$p - p_0 = M[-b(\epsilon - \epsilon^p) + (\phi - \phi^p)] \quad (27)$$

The plastic yield function is assumed to be given by the safe lower bound (7),

$$\sigma \in D'_{\text{hom}} \Leftrightarrow F(\sigma, p) = \max(f_I, f_M, f_{\text{int}}) \leq 0 \quad (28)$$

with the individual strength criteria given by:

$$f_{i=M, \text{int}}(\sigma, p) = \sqrt{J_2} + \delta_i [\sigma_m + b(p - p_0)] - k_i \quad (29)$$

and the flow rules, assumed to be associate:

$$d\epsilon^p = d\lambda \frac{\partial F}{\partial \sigma}; \quad d\phi^p = \frac{\partial F}{\partial p} = b d\epsilon^p \quad (30)$$

The material parameters of the model depend on the degradation state, or more precisely on the two parameters which govern the overall chemical damage mechanisms: the initial porosity  $\phi_0$  and the intrinsic chemical damage of the remaining solid phase, i.e.  $K_s$  or  $G_s$ :

- The drained elastic properties are defined by (10), which is similar in form to chemical damage models (cf. Gérard 1996; Gérard et al. 1996; Le Bellego 2001).
- The Biot parameters  $b = 1 - K_0/K_s$  and  $M = K_s/(b - \phi_0)$  are defined by (9), and the value of  $b$  increases from an initial value on the order of  $b = 0.1$  to unity. This parameter governs the pressure sensitivity of the degraded matter.
- The drained strength parameters  $\delta_i, k_i$  vary between the asymptotic values given in Table 1.

The model then appears as an (almost standard) multisurface poroplasticity model, and implementation of the model may well follow standard procedures of computational mechanics (Simo & Hughes 1998).

Figures 8 and 9 illustrate the predicted triaxial poroplastic strength behavior of the degraded cement paste specimens in the Mohr stress-plane (experimental results displayed in figure 2), the stresses being normalized by the compressive strength  $f'_c$ . As expected, the Mohr circles for drained experiments have an increasing diameter with increasing confinement pressure. The envelope with an initially constant slope starts flattening at confinement pressures greater than the uniaxial compression strength. The applied confinement pressures go up to twice the uniaxial strength of the degraded material. On the other hand, in the undrained case, displayed in figure 9, all the tests at different confinement pressure levels are, in terms of effective stress, only one triaxial test equivalent to the uniaxial compression test. This was confirmed experimentally by pore pressure measurements.

### 3.2 Deterioration Kinetics of Chemoplastic Softening

With the short-term behavior in hand, we are left with specifying the deterioration kinetics, i.e. the progress of the Calcium leaching fronts into the material bulk, which sets out the field condition of chemoplastic softening induced by Calcium leaching. The deterioration kinetics is

object of intensive research, ever since Adenot and Buil (1992) identified the multiple coupled diffusion-dissolution processes as critical for the long-term dimensional stability of material and structure (e.g., Adenot, 1992; Bentz & Garboczi

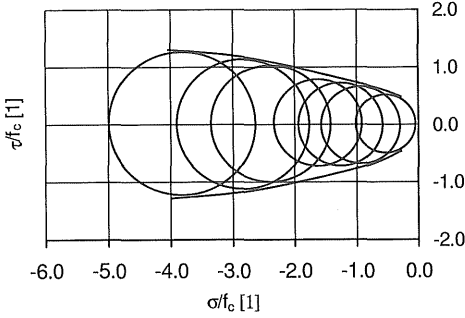


Figure 8: Drained poroplastic triaxial strength tests on calcium leached cement paste displayed in the Mohr stress-plane ( $p = p_0$ ).

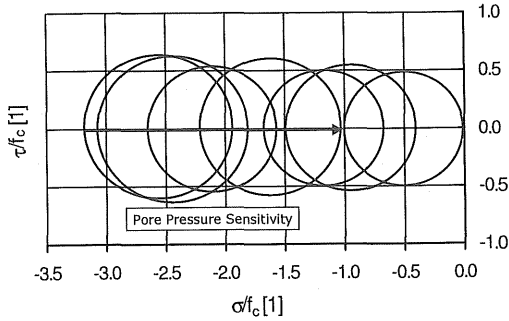


Figure 9: Undrained poroplastic triaxial strength results displayed in the Mohr stress-plane.

1992; Gérard 1996; Mainguy & Coussy, 2000; Le Bellego 2001). The deterioration kinetics is now well understood for uncracked concrete, for which it is governed by the classical square-root of time dependency of the diffusion problem, with dissolution fronts propagating at finite velocity into the structure bulk, i.e.  $x_d = \xi_d t^{1/2}$ , where  $\xi_d$  is an invariant, which depends only on a macroscopic solubility parameter of the substance involved in the dissolution process. On the contrary, for cracked porous media, there are two competing diffusion processes, one related to the diffusion of Calcium ions through the crack, the other to the diffusion through the bulk material. This leads for large times to a quadratic root of time dependency of the propagation front in the vicinity of cracks and fracture, i.e.  $x_d = \xi_d t^{1/4}$ , and the problem in time is scaled by the crack opening (Mainguy & Ulm 2001). The detailed derivation of the selfsimilarity properties of Calcium leaching in un-

cracked and cracked porous materials goes beyond our scope, and the interested reader is referred to Mainguy & Ulm (2001), Mainguy et al. (2001), Heukamp et al. (2001b) for details; but the overall emerging picture is that fractures with reasonable crack openings (e.g. shrinkage cracks), in which the mass transport is dominated by diffusion, do not significantly affect the overall deterioration kinetics: the large-time  $t^{1/4}$ -kinetics is slower than the  $t^{1/2}$ -kinetics characterizing the diffusion-dissolution process through the uncracked matrix. On the other hand, if convection dominates the mass transport in the fracture, an acceleration of the  $t^{1/2}$ -propagation may well occur, because the coupled convection-diffusion-dissolution process is also scaled by the square root of time.

Deterioration kinetics delivers the field conditions of the Calcium leaching in 'real' life structures, which are required to predict and anticipate the mechanical integrity of concrete structures. Given the slowness of the process, it is reasonable to assume drained pressure conditions at the time scale of the coupled diffusion-dissolution process (i.e.  $p = p_0$ ). As for skeleton evolutions, the problem reduces to one of an almost standard chemoplasticity model (Coussy & Ulm 1996), in which the strength and stiffness parameters evolve in time defined by the selfsimilar properties of the coupled diffusion-dissolution process (Ulm et al. 1999). The macroscopic strength domain can still be defined by the 'safe' lower bound (28), while the pore pressure is replaced by the chemoplastic hardening force  $\zeta$ :

$$\sigma \in D'_{\text{hom}} \Leftrightarrow F(\sigma, \zeta_i) = \max(f_I, f_M, f_{\text{int}}) \leq 0 \quad (31)$$

with:

$$f_{i=M,\text{int}}(\sigma, \zeta_i) = \sqrt{J_2} + \delta_i(\sigma_m + \zeta_i) - k_i \quad (32)$$

As the material is leached, the hardening force  $\zeta_i$  increases from a zero initial value to an asymptotic value,  $\zeta_i(\infty)$ , and in between these two limit states, the hardening force depends on the apparent Calcium concentration of the solid phase, i.e.  $\zeta_i = \zeta_i(s)$ . If we choose as reference state for chemical decohesion the unleached material, the asymptotic value,  $\zeta_i(\infty)$ , can be assessed from:

$$\zeta_i(\infty) = \frac{k_i(0) - k_i(\infty)}{\delta_i(\infty)} \quad (33)$$

together with a chemical softening function which accounts for the change in friction coefficient:

$$\frac{\delta_i(s)}{\delta_i(0)} = \mathcal{F}\left(\xi = \frac{s(t)}{s(0)}\right) \quad (34)$$

Function  $\mathcal{F}(\xi)$ , which is suggested to depend on

the normalized leaching degree  $\xi = \frac{s(t)}{s(0)}$ , varies between  $\mathcal{F}(1) = 1$  and  $\mathcal{F}(0) = \delta_i(\infty)/\delta_i(0)$ . For values given in Table 1 we obtain  $\zeta_M(\infty) = 64.3$  MPa and  $\mathcal{F}(0) = 0.28$  for the cement paste, and  $\zeta_{int}(\infty) = 11.8$  MPa and  $\mathcal{F}(0) = 0.66$  for the mortar. The difference in value of the asymptotic hardening force may well be attributed to the dominating role of the interfacial transition zone for mortars, while the difference in asymptotic frictional softening may well be scaled by the matrix volume fraction determining the apparent mineral concentration  $s$  in the mortar; but it is still too early to make definitive statements.

The previous equations focus on the material strength during chemoplastic softening. We may want to complete the chemoplasticity model by adding plastic hardening-softening phenomena, through the flow and hardening rules:

$$d\epsilon^p = d\lambda \frac{\partial F}{\partial \sigma}; \quad d\phi^c = \frac{\partial F}{\partial \zeta} = d\epsilon^p \quad (35)$$

where  $\phi^c = \epsilon^p$  is identified as the hardening variable, entering the hardening force:

$$\zeta_i = \zeta_i(\epsilon^p, \phi^c) \quad (36)$$

Finally, application of the consistency condition,  $dF = 0$ , delivers the plastic multiplier  $d\lambda$  and the plastic hardening modulus in the form (Coussy & Ulm 1996):

$$d\lambda = \frac{1}{H} \left[ \frac{\partial F}{\partial \sigma} : d\sigma + \frac{\partial F}{\partial \zeta} d\zeta \right] \quad (37)$$

$$H = - \left( \frac{\partial F}{\partial \zeta} \right)^2 \frac{\partial \zeta}{\partial \phi^c} = - [\delta_i(0) \mathcal{F}(\xi)]^2 h(38)$$

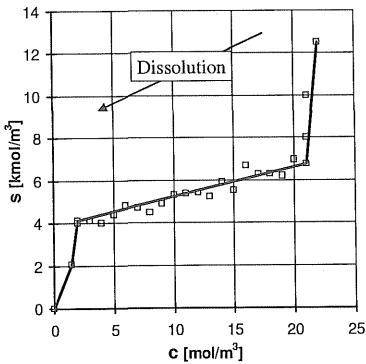


Figure 10: Chemical Equilibrium Condition between the apparent solid calcium concentration and the interstitial calcium concentration (sketched after Berner 1988).

The function  $h = \frac{\partial \zeta}{\partial \phi^c}$  represents pure plastic hardening or softening. If, for purpose of argument, we

assume that it is independent of the degradation state, i.e.  $h = h(\phi^c)$ , Eq. (38) shows that the hardening modulus may well depend on the leaching state; and the chemoplastic model, then, suggests that the absolute value of  $|H|$  reduces due to frictional softening, while the sign of plastic hardening depends only on the sign of function  $h(\phi^c)$ .

Last, the leaching state expressed by the leaching degree  $\xi = \frac{s(t)}{s(0)}$ , is related through a chemical equilibrium condition to the Calcium concentration  $c$  in the pore solution (see Figure 10):

$$s = g(c) \quad (39)$$

This chemical equilibrium condition is well known (Berner 1982; Gérard 1996), and provides the link between the mechanical problem and the deterioration kinetics. The chemoplastic model is then complete.

#### 4 CONCLUDING REMARKS

Durability Mechanics of Calcium leached cementitious materials allows for some interesting comparison with osteoporotic bone:

1. Calcium leaching in cementitious materials results from a difference in chemical potential between the calcium in the interstitial pore solution, and the calcium bound in the solid phase. The calcium in the pore solution is in contact with the calcium concentration in the environment. A mineral dissolution process (hydroxyapatite) also occurs in the course of the remodeling cycle of bone, and is also governed by a difference in chemical potential, but the difference occurs between the chemical potential of the solid bone (which no doubt includes the free energy of the solid matter, i.e. strain energy), and the one generated locally by osteoclasts in an acidic micro-subsurface environment occupied by the cells. This biologically generated potential (BGP), which is often referred to as biological pump, may well depend on hormones, and other biochemical control-cycles in the body. It affects the overall kinetics imbalance between resorption and refilling, and thus the decrease of bone mass density, leading to Osteoporosis.
2. Calcium leaching leads to an increased pressure sensitivity of cementitious materials, and an almost complete loss of frictional performance under undrained conditions. This is due to an increase in porosity and an intrinsic chemical damage of the remaining solid, and needs to be considered when designing leached structures for fast loading conditions (e.g. drop of a container). The reduced bone mass density of osteoporotic bone is an in-

dication that similar processes take place in bone; but it is still not clear whether an increase in pressure sensitivity during downfall, contributes to the higher risk of bone fracture. At present, it is argued that a change in the morphology of the microstructure, in addition to an increase in porosity, plays a critical role on the mechanical performance. Still, it appears that the mechanical performance may well be captured by a poroplastic approach, developed on similar lines of arguments as presented for the calcium leaching problem.

3. Calcium leached materials exhibit decohesion and frictional softening, but still they have a finite accountable strength, which may well be above either the weaker particulate (i.e. sand) or matrix (i.e. cement paste) strength. Hence, it can be taken into account in design and operation of critical infrastructure subjected to calcium leaching, including engineering health monitoring systems of critical infrastructure. This residual strength domain is surely critical when it comes to evaluating the risk of fracture of osteoporotic bone.

#### ACKNOWLEDGMENTS

This research was performed as part of Grant No. DE-FG03-99SF21891/A000 of the US Department of Energy (DOE) to MIT. The authors gratefully acknowledge the support of this work by the Nuclear Energy Research Initiative Program of DOE, and the collaboration with the Commissariat à l'Etude Atomique (C.E.A., Saclay, France), through Dr. Jérôme Sercombe.

#### REFERENCES

- Adenot, F. & Buil, M. (1992). Modelling of the corrosion of the cement by deionized water. *Cem. Concr. Res.*, 22(4), 451-457.
- Adenot, F. (1992). Durabilité du béton : caractérisation et modélisation des processus physique et chimiques de dégradation du ciment. Université d'Orléans, PhD Thesis.
- Berner, U. (1988). Modelling the incongruent dissolution of hydrated cement minerals. *Radiochimica Acta* (44), 387-393.
- Bentz, D.P., & Garboczi, E.J. (1992). Modelling the leaching of calcium hydroxide from cement paste: effects on pore space percolation and diffusivity. *Materials and Structures, RILEM*, Vol. 25, 523-533.
- Carde, C. (1996). Caractérisation et modélisation de l'altération des propriétés mécaniques due la lixiviation des matériaux cimentaires. INSA de Toulouse, Ph.D. Thesis.
- Carde, C., François, R., & Torrenti, J.M. (1996). Leaching of both calcium hydroxyde and C-S-H from cement paste: modeling the mechanical behaviour. *Cem. Concr. Res.*, 26(8), 1257-1268.
- Coussy, O. (1995). *Mechanics of porous continua*. John Wiley & Sons, Chichester, UK.
- Coussy, O. & Ulm, F.-J. (1996). Creep and plasticity due to chemo-mechanical couplings. *Archive of Applied Mechanics*, 66, 523-535.
- Da Re, G. (2000). Physical mechanisms controlling the pre-failure stress-strain behavior of frozen sand. MIT, Cambridge, Sc.D.-thesis.
- de Buhan, P. & Taliercio, A. (1991). A homogenization approach to the yield strength of composite materials. *Eur. J. Mech., A/Solids*, 10, no. 2, 129-154.
- Gérard, B. (1996). Contribution des couplages mécaniques-chimie-transfert dans la tenue à long terme des ouvrages de stockage de déchets radioactifs, Ecole Normale Supérieure de Cachan, PhD Thesis.
- Gérard, B., Pijaudier-Cabot, G., and Laborderie, Ch. (1998). Coupled diffusion damage modeling and the implications on failure due to strain localisation. *Int. J. Solids and Structures*, Vol. 35, n° 31-32, 4107-4120.
- Hellmich, Ch. & Ulm, F.-J. (2001). Hydroxyapatite concentration is Uniform in the Extra-Collagenous Ultrastructure of Mineralized Tissue. *J. of Biomechanics*, submitted.
- Heukamp, F.H., Ulm, F.-J. & Germaine, J.T. (2001). Mechanical Properties of calcium leached cement pastes: Triaxial stress states and the influence of the pore pressure. *Cement and Concrete Research*, in press.
- Heukamp, F.H., Mainguy, M. & Ulm, F.-J. (2001). Beyond the crack size criterion: the effect of a fracture on calcium depletion of cementitious materials. *FramCos-IV*, (in this Volume).
- Ishai, O. & Bodner R. (1970). Limits of linear viscoelasticity and yield of a filled and unfilled epoxy resin. *Transactions of the Soc. Rheology*, 14(2), 253-273.
- Kendall, J., Howard, A.J., Birchall, J.D.(1983). The relation between porosity, microstructure and strength, and the approach to advanced cement-based materials. *Phil. Trans. R. Soc. Lond., A* 310, 139-153.
- Le Bellégo, C. (2001) Couplages chimie-mécanique dans les structures en béton attaquées par l'eau: étude expérimentale et analyse numérique. Ecole Normale Supérieure de Cachan, PhD Thesis.
- Mainguy, M. & Coussy, O. (2000). Propagation Fronts During Calcium Leaching and Chloride Penetration, *Journal of Engineering Mechanics, ASCE*, 126(3), 250-257.

- Mainguy, M. & Ulm, F.-J. (2001). Coupled diffusion-dissolution around a fracture channel: the solute congestion phenomenon. *Transport in porous media*, in press.
- Mainguy, M., Ulm, F.-J., Heukamp, F.H. (2001). Similarity properties of demineralization and degradation of cracked porous materials. *Int. Journal of Solids and Structures*, in press.
- Simo, J.C. & Hughes, T.J.R. (1998). *Computational Inelasticity* (monograph). Springer, Berlin.
- Skempton, A.W. (1954). The pore-pressure coefficients *A* and *B*. *Geotechnique*, 3, 271–276.
- Ulm, F.-J., Torrenti, J.M., Adenot, F. (1999). Chemoporoplasticity of calcium leaching in concrete. *Journal of Engineering Mechanics*, ASCE, 125(10), 1200–1211.